EVALUATION OF COMBUSTION CHAMBER DESIGN USING CFD

MARTIN LISY, MICHAL SPILACEK, MAREK BALAS, ZDENEK SKALA

Energy Institute, Faculty of Mechanical Engineering, Brno University of Technology, Technická 2896/2, 616 69 Brno, Czech Republic

DOI : 10.17973/MMSJ.2019_06_201808

lisy@fme.vutbr.cz

This paper compares two designs of a gasification chamber for combustion of biomass from the view of combustion quality and the resulting gaseous emissions. To explain the difference in the emission values of the two different designs computational modeling is used to visualize basic processes important for combustion taking place in the combustion chamber, notably velocity field, temperature field and mass fractions of combustion air in assumed gasification products. Due to high computational demand, the model is heavily simplified, notably by the absence of chemical reactions between air and gasification products but is accurate enough for this study.

KEYWORDS

CFD, combustion, gasification, biomass, emissions

1 INTRODUCTION

The importance of biomass as a renewable energy source is growing each year, and one of the most explored technologies of biomass energy utilization is combustion. The resulting increase in the use of biomass for combustion goes hand in hand with requirements on improvements of relevant technologies due to more a more strict emission limits [Matus 2014]. One way to improve the combustion devices, that often use low-quality fuels with high water content, is the utilization of numerical models and computer modeling [Pospisil 2016]. This is an extremely versatile tool that, when mastered, can provide relevant and near real-life results that can be used for the enhancement of current design or even create entirely new ones without the need of building a device with such design first.

This paper deals with a very simplified numerical model and uses it to explain different emission results from two designs of one gasification chamber to verify if the said model is accurate enough and suitable for further expansion, most notably with chemical reactions.

2 DESCRIPTION OF THE DEVICE

The combustion device is utilized for combustion of loose biomass, such as wood chips and wood pellets at varying moisture content, from dry to very wet. The device is composed of four main parts (see Fig. 1): fuel feeder (5), gasification chamber (10), water heater (11) and air preheater (1, 2, 3, 4). Fuel from the fuel feeder is fed in the gasification chamber, where it is gasified and subsequently combusted. After combustion, the flue gas exits the gasification chamber in the form of (ideally) inert hot gas and enters the water heater. For this article, only the gasification chamber and the air preheater are important and described further in greater detail. A detailed description of the entire device can be found elsewhere [Spilacek 2014]. The nominal heat output of the device is 110 kW.

Gasification Chamber. The gasification chamber is designed with the high volatility of the biomass that it thermally converts in mind and the construction allows for gasification of fuel into syngas and subsequent complete combustion of the syngas. The process of gasification takes place on an inclined fixed grate. The fuel is fed in the chamber from the backside, falls on the inclined grate, and slides on it due to new fuel push and gravitational pull. From below of the inclined grate is introduced the primary that heats, dries and gasifies the fuel. Downwind, at the bottom of the inclined grate is a horizontal grate whose purpose is burnout of any fuel that was not gasified and removal of ashes. After the fuel is converted into syngas, secondary air can be introduced in the stream to commence an intense combustion. After this optional combustion, the resulting hot gas exits the gasification chamber via a channel in which a tertiary air, if needed, can be introduced into the gas stream. After leaving the combustion chamber, it then enters the water heater, see Fig. 2.

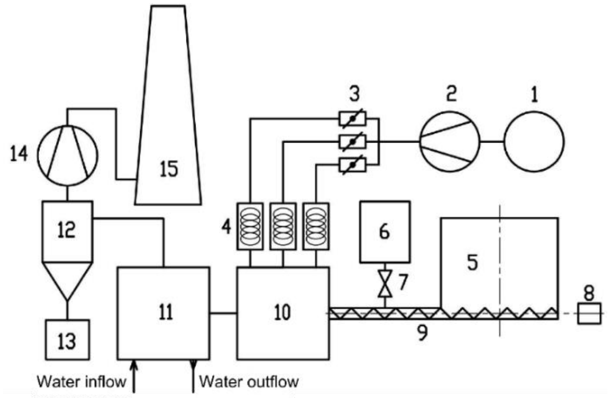

Figure 1. Experimental device – diagram [Spilacek 2014]

Air Preheater. Another important component of the device is its air preheater that divides by flaps the combustion air into three separated streams. Each of the stream flows is regulated separately as well as its temperature and can be preheated up to 200 °C. A ventilator provides the air.

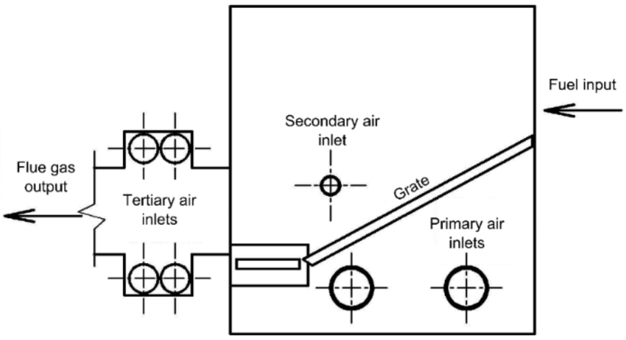

Figure 2. Combustion chamber – diagram [Spilacek 2014]

2.1 Numerical *model*

Combustion Air. Achieving complete combustion that results in high efficiency and low emissions is a very difficult task [Moskalik 2012]. Each stage of combustion requires a different amount of combustion air that must be introduced to the fuel and volatiles for long enough time and must be allowed to be mixed thoroughly [Lisy 2005]. And even when all this is provided, the resulting flow can have a negative influence on other processes of the combustion process, such as cooling of walls or high-pressure losses [Pospisil 2015]. A previous attempt tried to describe the velocity field [Spilacek 2016] with some success (see Fig. 3), but a more thorough study is needed to address the importance of temperature and mixing of syngas and combustion air.

Revisited Numerical Model. In this study, the geometry from the previous study (see Fig. 4) has been altered to only account for the volume above the grate, and the fuel feeding channel has also been removed. Currently, the assumption is that there is a uniform normal mass inflow from the entire area of the grate surface and the secondary air inlet, meaning there are two distinct inlets. The first is the grate area for the mixture of pyrolysis syngas and primary air – called the **grate gas** for this paper – and the second inlet is for the secondary air. This model also includes the acceleration of gravity and cooling of walls by natural convection. Chemical reactions are not considered.

Original design. Grate area inlet: For simplification of calculation and geometry, the assumption for the grate area inlet is that all the fuel is pyrolyzed (gasified without air) and perfectly premixed with primary air and the resulting mixture – grate gas – creates an ideal uniform normal pointwise mass flux over the entire grate area. The grate gas is considered to be ideal gas with temperature 800 °C that is in the actual range of gasification of biomass [Jelemensky 2013]. The grates gas' mass flow is affected by its density, which depends on pressure and temperature.

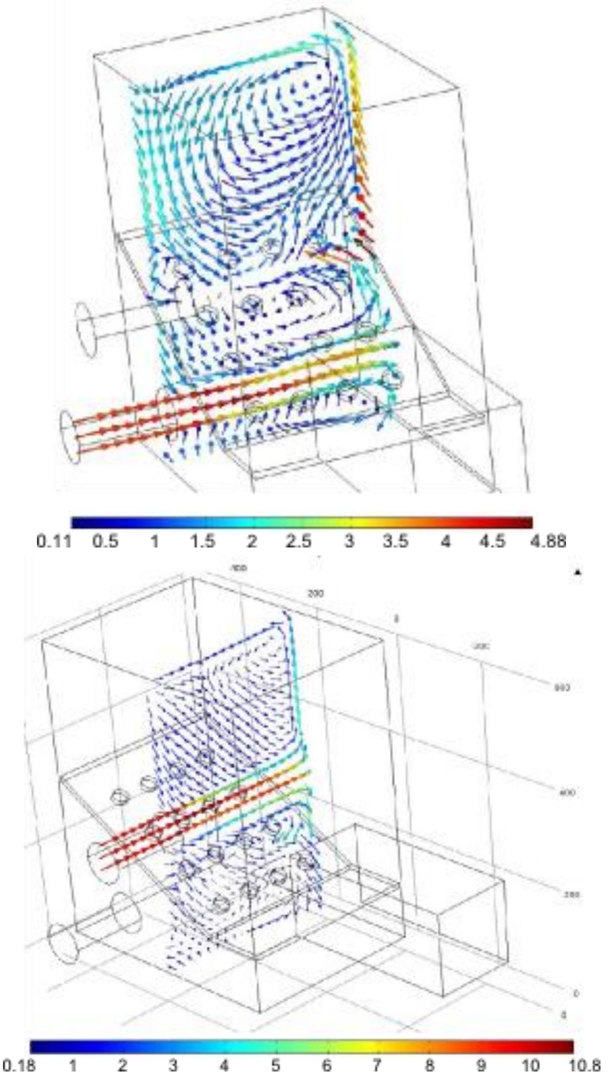

Figure 3. Selected results of velocity field from previous study [Spilacek 2016]

The amount of mass entering the model from the grate area is calculated from the composition of a pyrolysis syngas, see Tab. 1, and from the amount of primary air. The molar mass of the syngas is calculated for an ideal gas:

$$m_{syn}=\sum_i M_i \cdot x_i \text{ [g/mol]} \quad (1)$$

Where:

Mi... molar mass of the ith component [g/mol],

xi… volume fraction [-].

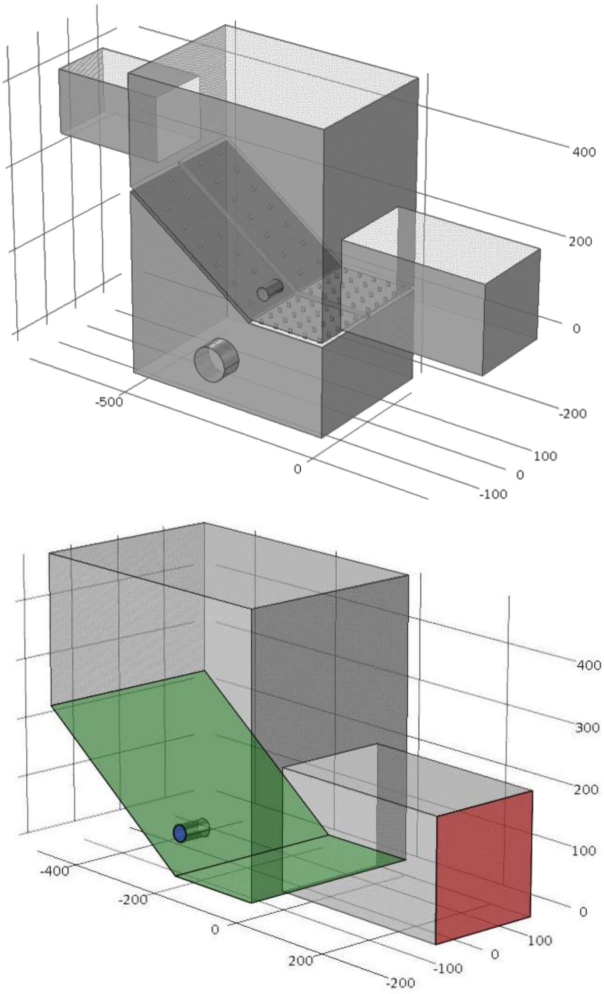

Figure 4. Original and revisited geometry. Green – grate gas inlet. Blue – secondary air inlet, Red – exit surface (outlet)

C	H_2	CO	CO_2	CH_4	O_2	N_2
M_i	2.016	28.010	44.010	16.042	32.000	28.016
X_i	10.0	13.1	15.6	0.8	0.5	60.0

Table 1. Composition of a pyrolysis syngas, C means Compound, M_i in g/mol, X_i is dimensionless [Lisy 2005]

The resulting molar mass of the syngas is 27.384 g/mol.

The amount of produced syngas depends on the amount of fuel utilized in the device. The values for this device are available from [Kois 2014] and tabulated in Tab. 2.

From equation (2), the mass flow of primary air is:

$$m_{1^\circ} = k_1 \cdot m_{air} \cdot m_f \ \text{[kg/s]} \quad (2)$$

$$m_{1^\circ} = 3.65 \cdot 10^{-2} \text{ kg/s}$$

After adding up the amount of syngas produced from fuel reduced by ash content, the total mass flow of the **grate gas** from the grate area is:

$$m_1 = (1-A^r) \cdot m_f + m_{1^\circ} \ \text{[kg/s]} \quad (3)$$

$$m_1 = 14.14 \cdot 10^{-2} \text{ kg/s}$$

Fuel mass flow	mf [kg/s]	1.05e-2
Required air for combustion	m_{air} [kg/kgf]	8.69
Portion of primary air	k_{1° [-]	0.4
Ash content	A^r [-]	7.71e-3

Table 2. Values for fuel and primary air of the device

Secondary air inlet: The mass flow of the secondary air is equal to the difference between the required amount of combustion air and primary air. The secondary air is preheated to 199.5 °C, and its molar mass is 28.964 g/mol.

$$m_2 = (1-k_{1^\circ}) \cdot m_{air} \cdot m_f \ \text{[kg/s]} \quad (4)$$

$$m_2 = 5.47 \cdot 10^{-2} \text{ kg/s}$$

Emission results of the original design. The emissions were measured for three combustion regimes of different combustion air temperatures and each for two different moistures of biomass in the flue gas duck between the parts 11 and 12, see Fig. 1. The measured emissions were carbon monoxide (CO) and nitrogen oxides (NO_X). The content of oxygen was also measured for reference. The results are shown in Tab. 3.

T_{air}	Water content: 35 %			Water content: 55.8 %		
	CO_{ref}	NO_{Xref}	O_2	CO_{ref}	NO_{Xref}	O_2
25	2,039	82	11.3	19,598	147	14.1
100	1,030	95	11.3	9,535	88	9.6
200	1,071	102	11.7	4,683	105	14.1

Table 3. *Emission results of the original design of the chamber, CO and NO_{xref} in mg/m^3, O_2 in %, T_{air} in °C [Zboril 2014]*

Improved design. To improve the original design, a screen was installed in the chamber (Fig. 14 and Fig. 15). This provided a change for all the 3 Ts – Time, Temperature and Turbulence – physical effects that have the most important impact on the quality of combustion. The impact of this change can be seen in Tab. 4. When compared with the emission results of the original design (Tab. 3), it is clear that the improved design has significantly lowered the emissions of carbon monoxide, while the emissions of nitrogen oxides raised only slightly.

The strictest legislative limits according to ČSN-EN 303-5 and regulation 415/2012 Sb. for a device with such power output are 500 mg/m³ CO and 600 mg/m³ NO_X for the reference amount of oxygen 10 %. While both the original and improved design meets the limits for nitrogen oxides, only the improved design was able to meet the limits for carbon monoxide and only for lower water content in the fuel.

These emission results provide good diversity for further investigation into how has the improved design changed the 3 Ts and can help to verify the numerical model.

T_{air}	Water content: 35 %			Water content: 55.8 %		
	CO_{ref}	NO_{Xref}	O_2	CO_{ref}	NO_{Xref}	O_2
25	149	104	11.4	1,445	181	12.2
100	147	95	11.9	1,584	175	12.6
200	192	98	12.5	1,008	188	12.1

Table 4. *Emission results of the improved design of the chamber, CO and NO_{xref} in mg/m^3, O_2 in %, T_{air} in °C [Zboril 2014]*

3 RESULTS

3.1 Original design

Velocity: The velocity field shows that the chamber has a good potential for mixing of volatiles and combustion air. A vortex that goes all the way from the end of the fuel feeding channel to the exit channel provides great turbulence that is necessary for good mixing. However, the speed of the secondary air is a problematic element, since it hits the opposite wall directly, cooling it down and then long going around the top and other walls, not participating in the mixing process, see Fig. 5 and Fig. 6. Another problematic element is the direct escape of the mixture from the grate in the exit channel that is clearer from temperature results.

This model provides a more detailed look than the previous one [Spilacek 2016].

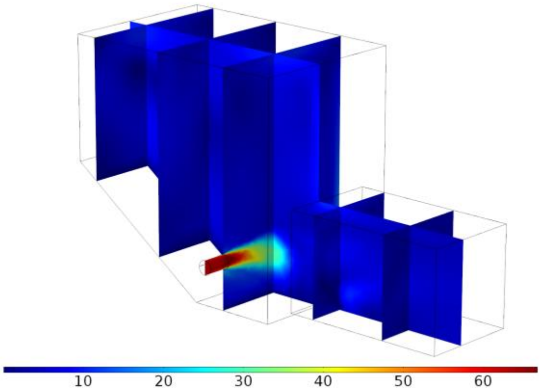

Figure 5. Velocity field [m/s] in the chamber, original design

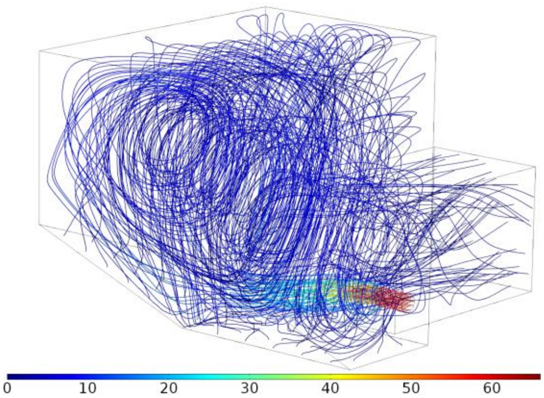

Figure 6. Velocity streamlines [m/s] in the chamber, original design

Temperature: The temperature results show that the cooling of walls and early escape are present. However, the escape occurs mainly from the horizontal grate that is supposed not to have any volatiles or combustible matter left. Cooling of walls is a real issue with this design, see Fig. 7 and Fig. 8, but the escape of unmixed secondary air with the grate mixture will be better observable in the mass fraction results. The maximum and minimum temperature at the exit surface is 679.30 °C and 335.21 °C respectively.

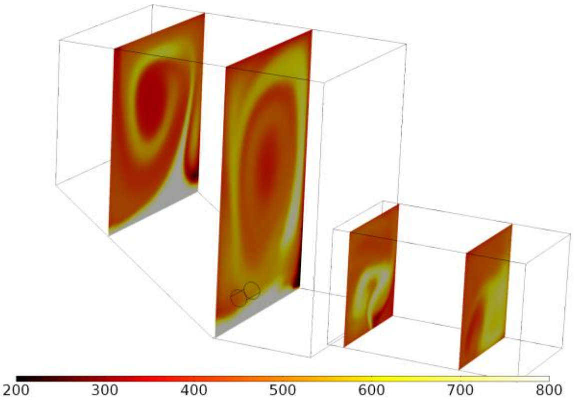

Figure 7. Temperature field [°C] in the chamber, original design

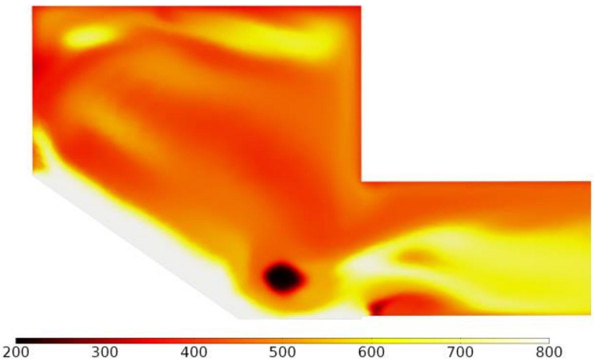

Figure 8. Temperature [°C] slice at the symmetry plane, original design

Mass fraction: From the resulting mass fraction of the mixture, it is clear that it is fairly well mixed with the secondary air and that the unmixed part in the exit channel results mostly from the horizontal grate, creating an uneven mixture at the exit of the chamber (see Fig. 11). It is also clear that the secondary air lingers for a long time at the walls, rendering the mixing capacity of this design suboptimal, with the maximum value 0.73 and minimum 0.51 mass fraction of the grate gas at the exit surface. The mass fraction is shown in Fig. 9, Fig. 10 and Fig. 11.

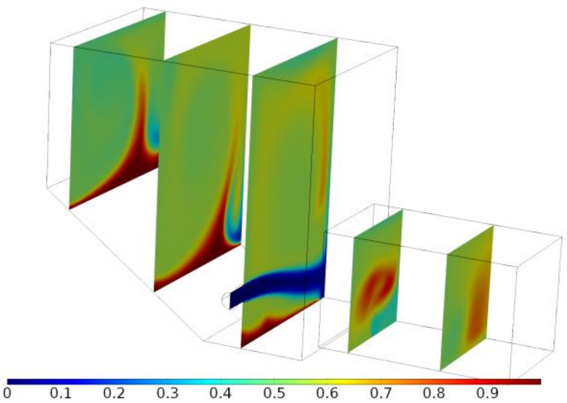

Figure 9. Mass fraction of the grate gas in the original chamber

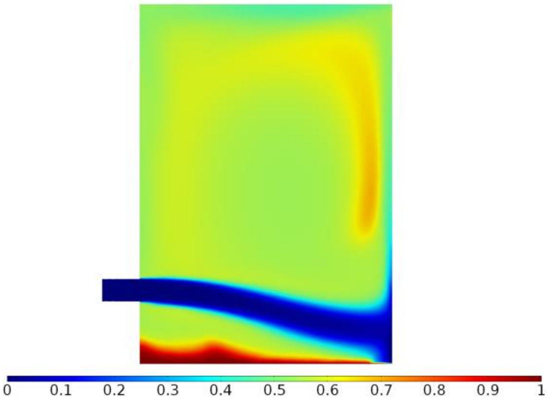

Figure 10. Mass fraction of the grate gas in slice at the secondary air inlet, original design

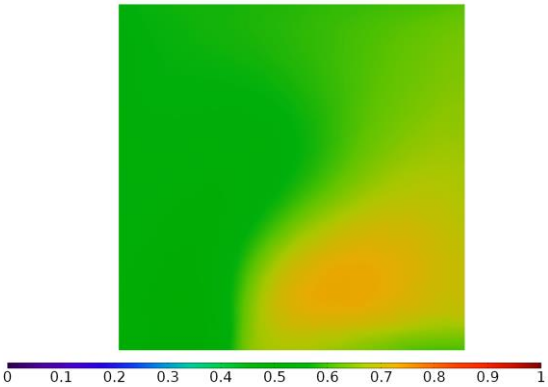

Figure 11. Mass fraction of the grate gas at the exit surface, original design

3.2 Improved design

Velocity: The velocity field of the improved design is very different. There is no great vortex in the chamber, but two smaller ones instead. One is under the screen near the wall opposing the combustion air inlet going alongside the grate and the second vortex is above the screen with its axis parallel to the axis of the combustion air inlet. The direct escape of the mixture does not occur, and the washing of the opposite wall is greatly diminished. But a new problematic region is located in the exit nozzle that now doesn't have an appropriate geometry for the flow and results in its cooling. See Fig. 12 and Fig. 13.

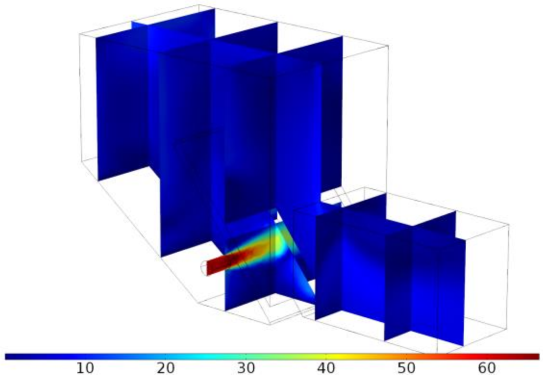

Figure 12. Velocity field [m/s] in the chamber, improved design

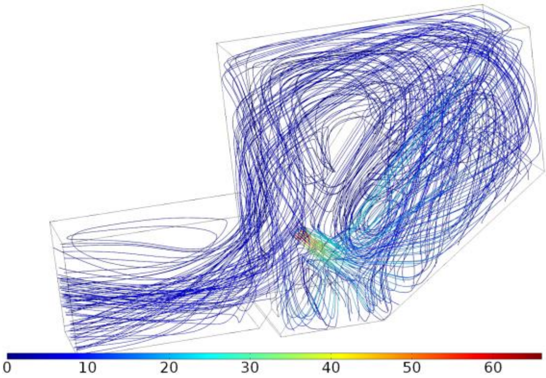

Figure 13. Velocity streamlines [m/s] in the chamber, improved design

Temperature: The temperature field of the improved design is much more uniform in the main volume of the chamber than the one of the original design, but is still hampered by an unsuitable geometry of the exit nozzle resulting in superfluous cooling, with maximum 679.51 °C and minimum 347.40 °C at the exit surface. The lower value is probably caused by creeping of the secondary air alongside the wall. This is still an overall improvement, and even the cooling of the walls is smaller, see Fig. 14 and Fig. 15.

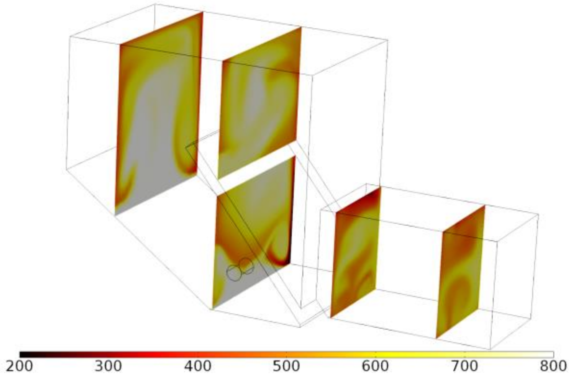

Figure 14. Temperature field [°C] in the chamber, improved design

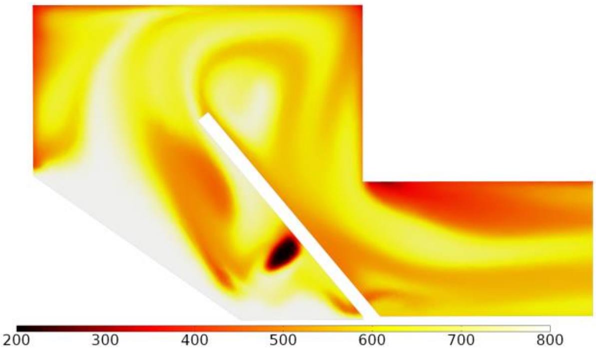

Figure 15. Temperature [°C] slice at the symmetry plane, improved design

Mass fraction: The mixing of the two gases in the chamber is better with the improved design. Even though the velocity field suggests lower mixing rate, the extended length at which the two gases are mixing results in an almost complete mixing with minimum value 0.62 and maximum 0.70 mass fraction of the grate gas at the exit surface, see Fig. 16, Fig. 17 and Fig. 18. The difference of the final mixing quality can be seen when comparing Fig. 11 and Fig. 18.

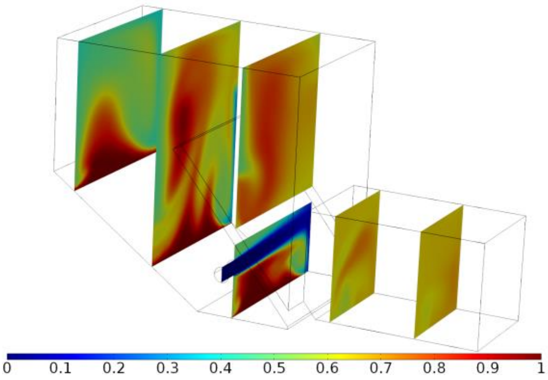

Figure 16. Mass fraction of the grate gas in the chamber, improved design

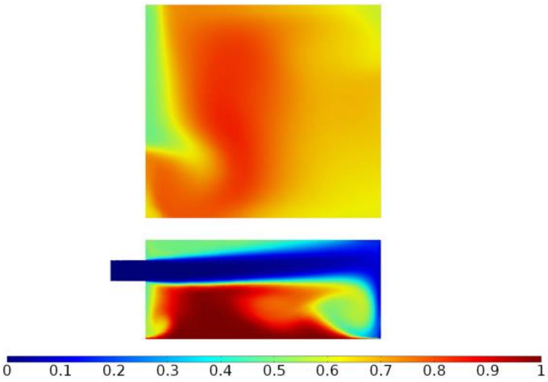

Figure 17. Mass fraction of the grate gas in a slice at the secondary air inlet, improved design

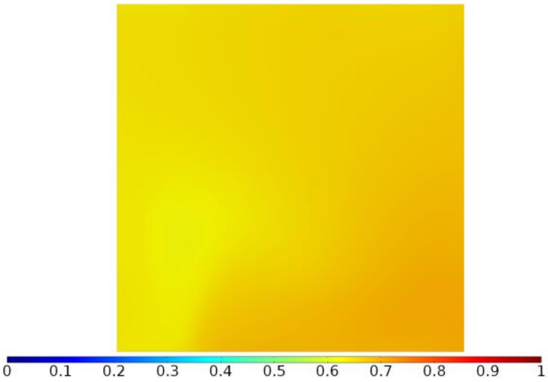

Figure 18. Mass fraction of the grate gas at the exit surface, improved design

4 CONCLUSIONS

The results from the updated numerical model that includes velocity, temperature, and mass fraction study make a detailed overview of the processes that occur in the combustion chamber. The chamber's original design is suboptimal mostly from the time the secondary air lingers alongside the walls, cooling them and not mixing with the combustible syngas. The numerical model can visualize the basic problems of that design and why it has such high emissions of carbon monoxide and lower emissions of nitrogen oxides due to low mixing of volatiles with combustion air and an uneven temperature field.

Many of the mentioned problems are avoided in the improved design. Here, the numerical model can also visualize and explain why the emissions of carbon monoxide are much lower, and those of nitrogen oxides are slightly higher. Mixing of volatiles with combustion air, while the turbulence is not as great as in the original design, takes longer time and in the entire volume of the chamber. This means the conditions for chemical reactions in the gas that reduce carbon monoxide but also produce nitrogen oxides last longer. The temperature field is also much more uniform in the main volume of the chamber, but still suboptimal in the exit nozzle.

The presented numerical model has many simplifications and assumptions that may adversely affect the results, notably the absence of chemical reactions and direct convection at walls, and therefore it did not provide exact results for controlled emissions. But this was not the aim of this study. The main aim was to verify if the numerical model can explain the different emissions results according to contemporary theories of combustion. The model seems to be capable of that, and the issues of chemical reactions will be addressed in further studies.

ACKNOWLEDGMENTS

This work was supported by the Ministry of Education, Youth and Sports of the Czech Republic under OP RDE grant number CZ.02.1.01/0.0/0.0/16_019/0000753 "Research centre for low-carbon energy technologies".

REFERENCES

[Jelemensky 2013] Jelemensky L., Gasparovic, L., Markos, J. Biom*, České sdružení pro biomasu*, 2013, Biom.cz [online]. 20. 5. 2013 0 [02. 05. 2018]. Available from <https://biom.cz/cz/odborne-clanky/energeticke-vyuzitie-rastlinnej-biomasy-2-termicke-procesy>. ISSN: 1801-2655.

[Kois 2014] Kois, J. Computational Model of KWH Boiler. Location: Brno University of Technology, Faculty of Mechanical Engineering, Brno, 2014.

[Lisy 2005] Lisy, M., Balas, M., Kohout, P. Energetic parameters of biomass during fluid bed combustion. Energy from Biomass IV, 2005, pp 55-62, ISBN 80-214-3067-2.

[Matus 2014] Matus, M., Krizan, P., Soos, L., Beniak, J., Lisý, M.The influence of Size Fraction and Moisture Content on the Compressibility of Wood Sawdust in Effective Process of Production of Solid Biofuel, In International multidisciplinary geoconference SGEM. International multidisciplinary geoconference SGEM. 4. 2014. pp. 553-560 ISSN: 1314-2704.

[Moskalik 2012] Moskalik, J. Skvaril, J., Stelcl, O., Balas, M., Lisy, M. Energy recovery from Contaminated Biomass. Acta Polytechnica, 2012, vol. 52, n. 3, pp. 77-82. ISSN: 1210- 2709.

[Pospisil 2015] Pospisil, J., Lisy, M., Spilacek, M.: Mixing of flu-gas stream by local acceleration in channel of biomass boiler. In Reacent Advances in Environmental and Earth Sciences and Economic. Energy, Environmental and Structural Engineering. 1. Zakyntos, Řecko: WSEAS Press, 2015. pp. 345-350. ISBN: 978-1-61804-324- 5 ISSN: 2227- 4359.

[Pospisil 2016] Pospisil, J., Lisy, M., Spilacek, M.: Optimalization of Afterburner Channel in Biomass Boiler Using CFD Analysis. Acta Polytechnica, 2016, vol. 56, n. 5, pp. 379-387. ISSN: 1210-2709.

[Spilacek 2014] Spilacek, M. ANNALS of Faculty Engineering Hunedoara – International Journal of Engineering [online]. 02. 2014, volume Nr 12., issue Nr. 1, 02. 2014 [02. 05. 2018]. Available from < annals.fih.upt.ro/pdf-full/2014/ANNALS-2014-1-09.pdf >. ISSN: 1584-2673.

[Spilacek 2016] Spilacek, M., Lisy, M., Skala, Z. Numerical Study of Air Distribution in Combustion Chamber. Applied Mechanics and Materials, 2016, Vol. 832, pp 218-223.

[Zboril 2014] Zboril, M. Re-design of biomass boiler for very wet fuel. Location: Brno University of Technology, Faculty of Mechanical Engineering, Brno, 2014.

CONTACTS:

Ing. Martin Lisy, Ph.D.
Brno University of Technology, Faculty of Mechanical Engineering, Energy Institute
Technicka 2896/2, Brno, 616 69, Czech Republic
+420 54114 2582, lisy@fme.vutbr.cz, https://www.vutbr.cz/lide/martin-lisy-14231